

Low-loss hybrid plasmonic waveguide for compact and high-efficient photonic integration

Yao Kou, Fangwei Ye, and Xianfeng Chen*

Department of Physics, The State Key Laboratory on Fiber Optic Local Area Communication Networks and Advanced Optical Communication Systems, Shanghai Jiao Tong University, Shanghai 200240, China
*xfchen@sjtu.edu.cn

Abstract: A new hybrid plasmonic waveguide is introduced and characterized in the paper. By coupling the photonic modes of a Si waveguide with the higher-order plasmonic modes of a silver nanowire, we demonstrate that the resultant hybrid modes possess small mode areas and long propagation distances, as well as high excitation efficiency (~90%) from the conventional dielectric modes. Such hybrid waveguides may find applications in the high-dense photonic integrations.

©2011 Optical Society of America

OCIS codes: (240.6680) Surface plasmons; (250.5300) Photonic integrated circuits

References and links

1. R. Charbonneau, N. Lahoud, G. Mattiussi, and P. Berini, "Demonstration of integrated optics elements based on long-ranging surface plasmon polaritons," *Opt. Express* **13**(3), 977–984 (2005).
2. P. Berini, "Plasmon-polariton modes guided by a metal film of finite width bounded by different dielectrics," *Opt. Express* **7**(10), 329–335 (2000).
3. J. Dionne, L. Sweatlock, H. Atwater, and A. Polman, "Plasmon slot waveguides: Towards chip-scale propagation with subwavelength-scale localization," *Phys. Rev. B* **73**(3), 035407 (2006).
4. T. Holmgaard and S. Bozhevolnyi, "Theoretical analysis of dielectric-loaded surface plasmon-polariton waveguides," *Phys. Rev. B* **75**(24), 245405 (2007).
5. V. S. Volkov, S. I. Bozhevolnyi, E. Devaux, J.-Y. Laluet, and T. W. Ebbesen, "Wavelength selective nanophotonic components utilizing channel plasmon polaritons," *Nano Lett.* **7**(4), 880–884 (2007).
6. J. Takahara, S. Yamagishi, H. Taki, A. Morimoto, and T. Kobayashi, "Guiding of a one-dimensional optical beam with nanometer diameter," *Opt. Lett.* **22**(7), 475–477 (1997).
7. E. Verhagen, M. Spasenović, A. Polman, and L. K. Kuipers, "Nanowire plasmon excitation by adiabatic mode transformation," *Phys. Rev. Lett.* **102**(20), 203904 (2009).
8. S. J. Al-Bader, "Optical transmission on metallic wires-fundamental modes," *IEEE J. Quantum Electron.* **40**(3), 325–329 (2004).
9. H. Dittlbacher, A. Hohenau, D. Wagner, U. Kreibitz, M. Rogers, F. Hofer, F. R. Aussenegg, and J. R. Krenn, "Silver nanowires as surface plasmon resonators," *Phys. Rev. Lett.* **95**(25), 257403 (2005).
10. J. Jung, T. Søndergaard, and S. Bozhevolnyi, "Theoretical analysis of square surface plasmon-polariton waveguides for long-range polarization-independent waveguiding," *Phys. Rev. B* **76**(3), 035434 (2007).
11. R. F. Oulton, V. J. Sorger, D. A. Genov, D. F. P. Pile, and X. Zhang, "A hybrid plasmonic waveguide for subwavelength confinement and long-range propagation," *Nat. Photonics* **2**(8), 496–500 (2008).
12. D. Dai and S. He, "A silicon-based hybrid plasmonic waveguide with a metal cap for a nano-scale light confinement," *Opt. Express* **17**(19), 16646–16653 (2009).
13. H.-S. Chu, E.-P. Li, P. Bai, and R. Hegde, "Optical performance of single-mode hybrid dielectric-loaded plasmonic waveguide-based components," *Appl. Phys. Lett.* **96**(22), 221103 (2010).
14. R. F. Oulton, V. J. Sorger, T. Zentgraf, R.-M. Ma, C. Gladden, L. Dai, G. Bartal, and X. Zhang, "Plasmon lasers at deep subwavelength scale," *Nature* **461**(7264), 629–632 (2009).
15. P. B. Johnson and R. W. Christy, "Optical constants of the noble metals," *Phys. Rev. B* **6**(12), 4370–4379 (1972).
16. Y. Yin, Y. Lu, Y. Sun, and Y. Xia, "Silver nanowires can be directly coated with amorphous silica to generate well-controlled coaxial nanocables of silver/silica," *Nano Lett.* **2**(4), 427–430 (2002).
17. R. Yang, R. A. Wahsheh, Z. Lu, and M. A. G. Abushagur, "Efficient light coupling between dielectric slot waveguide and plasmonic slot waveguide," *Opt. Lett.* **35**(5), 649–651 (2010).
18. L. Chen, J. Shakya, and M. Lipson, "Subwavelength confinement in an integrated metal slot waveguide on silicon," *Opt. Lett.* **31**(14), 2133–2135 (2006).
19. Z. Han, A. Y. Elezzabi, and V. Van, "Experimental realization of subwavelength plasmonic slot waveguides on a silicon platform," *Opt. Lett.* **35**(4), 502–504 (2010).
20. J. Tian, S. Yu, W. Yan, and M. Qiu, "Broadband high-efficiency surface-plasmon-polariton coupler with silicon-metal interface," *Appl. Phys. Lett.* **95**(1), 013504 (2009).
21. G. Veronis and S. Fan, "Theoretical investigation of compact couplers between dielectric slab waveguides and two-dimensional metal-dielectric-metal plasmonic waveguides," *Opt. Express* **15**(3), 1211–1221 (2007).

1. Introduction

Surface plasmon polaritons (SPP), due to its strong light confinement property, is considered as a promising solution in developing compact photonic devices and circuits. In the past years, a variety of plasmonic structures have been investigated, including long-range SPP (LRSP) [1,2], metal-insulator-metal (MIM) [3], dielectric-loaded SPP (DLSP) [4], V-groove waveguides [5] and metal nanowires [6–10]. However, due to the large ohmic loss of metals, all these waveguides suffer from a trade-off between the confinement ability and the propagation length. To avoid this problem to some extent, a hybrid waveguiding mechanism was proposed recently [11–13]. Such waveguides, usually composed of a high-index dielectric waveguide placed over the metal plain with a nano-scale low-index gap, support photonic-plasmonic hybrid mode, which offers tight energy confinement with a lower propagation loss. This property facilitates their practical use [14].

In this paper, we proposed a different type of hybrid plasmonic waveguide which is constructed by embedding a SiO₂-covered silver nanowire into a Si waveguide. Metal nanowires have unique advantages for building the integrated optical circuits due to their small size and flexible shape. Usually, studies are focused on the fundamental mode ($m = 0$ mode) of the nanowires because this mode has a strong confinement nature [6,7]. However, such a radially polarized mode also leads to significant propagation loss, especially when the nanowire size becomes small [6–8]. In this work, by coupling the photonic modes of Si waveguide with the $m = 1$ modes of the nanowire (instead of the fundamental plasmonic modes as usually did [11–14]), we demonstrate the formation of two orthogonal “linearly-polarized” hybrid modes. Such higher-order hybrid modes exhibit small mode areas with long propagation distances. Moreover, due to its “linearly polarized” nature, the hybrid mode displays a high coupling efficiency (~90%) when excited by conventional dielectric modes.

2. Waveguide structure and mode characteristics

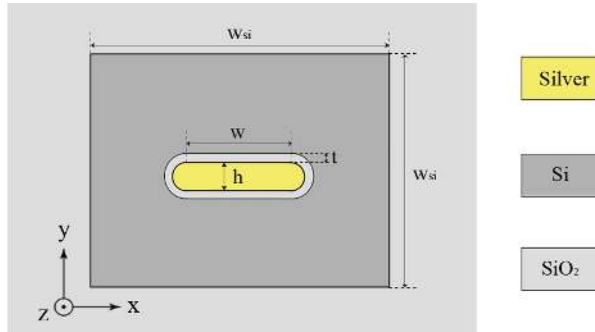


Fig. 1. Cross section of the present hybrid plasmonic waveguide.

The geometry of the proposed waveguide is illustrated Fig. 1. A silver nanowire, covered by a thin SiO₂ ($\epsilon_{\text{SiO}_2} = 2.25$) layer with thickness t , is embedded into a Si waveguide ($\epsilon_{\text{Si}} = 12.25$, $w_{\text{Si}} = 400$ nm). To ensure the formation of a hybrid mode, a substrate with lower index than that of Si should be used, as this is the prerequisite for the formation of the pure photonic modes, which might couple with the plasmonic modes and finally lead to the formation of hybrid modes. In our design, the whole structure is surrounded by a substrate which is also set to be SiO₂. In order to study the impact of geometry on the mode characteristics, the cross section of the nanowire is supposed to be a rectangular with width w and height h , which connects with two semi-circulars in the x direction. In the following discussions, h is fixed as 10 nm, whereas w increases from 0 to 100 nm. The choice of the Si waveguide dimension ensures that only the fundamental photonic modes can be supported in a pure Si waveguide with the same size. The operation wavelength is set to be $\lambda = 1550$ nm, corresponding to the permittivity of silver as $\epsilon_m = -129 + 3.3i$ [15]. The possible fabrication process of the

proposed structure is briefly described as follows: the silica-coated silver nanowire can be prepared through a sol-gel process [16]. Then it should be spin-coated onto an alpha-Si film with a suitable thickness, which is obtained by the plasma enhanced chemical vapor deposition (PECVD). With the e-beam lithography the lower half the Si waveguide is able to be fabricated, followed by a PECVD to form the upper half of the Si waveguide. The surrounding SiO₂ substrate can also be deposited using the PECVD. All the numerical calculations given below are based on finite element software COMSOL Multiphysics. The mode calculations are implemented in a square computation window with scattering boundary condition. The size of the window is set as 10-20 μm to ensure that the mode field is close to zero at the boundaries so that the influence of truncation can be avoided. Small enough mesh is used at the fine structures and the computation accuracy is guaranteed by the convergence analysis. The propagation length of a mode is given by $PL = \lambda/[4\pi\text{Im}(N_{\text{eff}})]$, where N_{eff} is the effective index. The normalized mode area is denoted as A_m/A_0 , where $A_0 = \lambda^2/4$ is the diffraction-limited area and A_m the ratio of the total mode energy to the peak energy density [11]:

$$A_m = \frac{\int_{A_\infty} W(\mathbf{r}) dA}{\max\{W(\mathbf{r})\}} \quad (1)$$

$$W(\mathbf{r}) = \frac{1}{2} \left(\frac{d(\varepsilon(\mathbf{r})\omega)}{d\omega} |E(\mathbf{r})|^2 + \mu_0 |H(\mathbf{r})|^2 \right) \quad (2)$$

Before we study the hybrid modes in our structure, we first have a look at the pure plasmonic modes supported by a pure nanowire. When the transverse dimension of a nanowire is reduced into a deep-subwavelength scale, only the fundamental mode ($m = 0$ mode) [Fig. 2(a)] and the two orthogonal polarized higher-order modes ($m = 1$ modes) [Fig. 2(b) and (c)] survive. The $m = 0$ mode exhibits a large effective index and a tight confinement, however, also a large attenuation. In contrast, the $m = 1$ modes feature low loss but with large mode sizes (more than several micrometers as the dimension of the nanowire goes below 100 nm [8,10]).

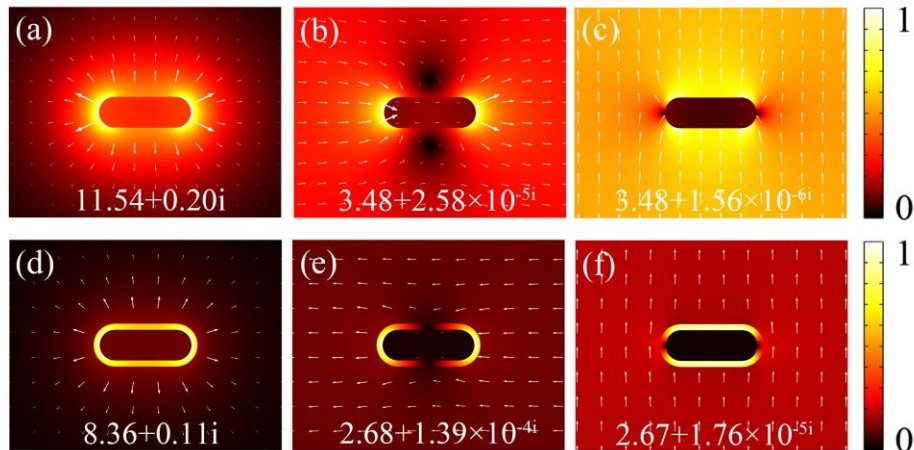


Fig. 2. $|E|$ distribution of the guiding modes supported by the pure silver nanowire surrounded by Si with $w = 20$ nm (a)-(c), and by the proposed hybrid plasmonic waveguide with $w = 20$ nm and $t = 2$ nm (d)-(f). The white arrows represent the orientation of the electric field. The effective refractive index of the modes is also shown in the figures.

With our hybrid structure, there also exist three modes. The first mode [Fig. 2(d)], having its electric field centrosymmetrically oriented, corresponds to the fundamental mode in a pure nanowire discussed above. Although the field is well confined in the SiO₂ layer (with a

normalized mode area on the order of 10^{-2}), its application is in question since its typical propagation length is only less than $10\ \mu\text{m}$. Moreover, when connected with other types of dielectric/plasmonic waveguides, such a radial polarized mode could also have a poor coupling efficiency due to polarization mismatch.

Besides the fundamental mode, Figs. 2(e) and (f) show two “higher-order hybrid (HOH) modes” that the proposed structure supports. In the Si region, the electric field of the hybrid modes resembles the pure photonic modes and has a linear polarization in the Si waveguide. However, in the $\text{SiO}_2/\text{silver}$ region, it resembles higher-order plasmonic modes which are “quasi-linearly” polarized near the silver core. The formation of these HOH modes can be regarded as the coupling between the x -polarized (y -polarized) fundamental photonic mode of the Si waveguide and the plasmonic $m = 1$ mode of the silver nanowire. We denote them as H_x^1 mode and H_y^1 mode, respectively, where H represents hybrid mode, the superscript indicates $m = 1$ plasmonic mode and the subscripts indicate the polarization. It is generally believed that the confinements of the higher-order modes are much weaker than that of the fundamental ones and are thus discarded in the considerations. However, as we shown that, the H_x^1 mode and H_y^1 mode are still well confined within the SiO_2 layer, despite their higher-order mode nature. This can be understood from their field profiles as shown in Figs. 2(e) and (f): close to the silver nanowire, the polarization of the dominant electric field component is always perpendicular to the metallic surface and thus features the high confinement within the lower-index SiO_2 layer. Calculation shows that the normalized mode area of the HOH modes is on the order of 10^{-1} , depending on w and t (shown later). On the other hand, the propagation loss of the HOH modes is greatly improved in comparison with the fundamental mode. With proper structural parameters, both the HOH modes can travel longer than $1\ \text{mm}$. Therefore, HOH modes are characterized by both a strong confinement and a long propagation distance, and thus meet the requirements for the compact photonic integrations.

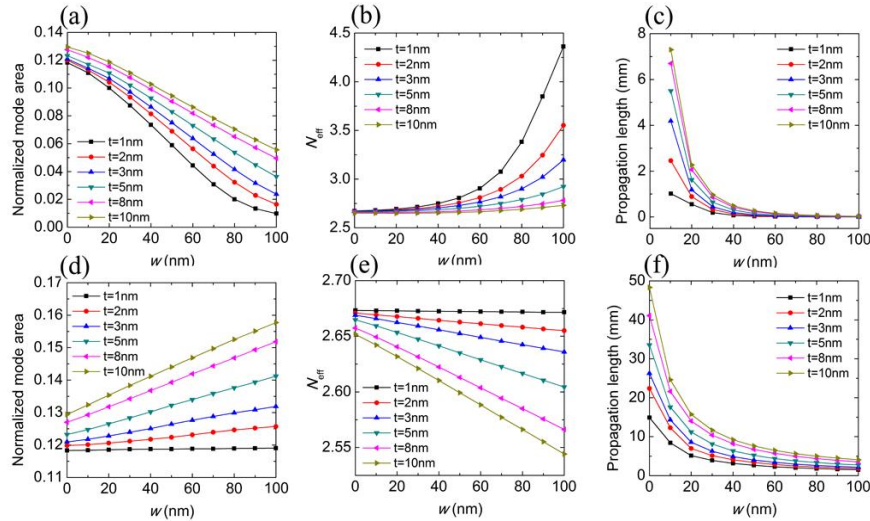


Fig. 3. Mode characteristics of the H_x^1 mode (a)-(c) and the H_y^1 mode (d)-(f) as a function of core width w with different SiO_2 thickness t .

Figure 3 plots the normalized mode area (MA), the real part of effective refractive index (N_{eff}) and the propagation length (PL) of the HOH modes as a function of w and t . For H_x^1 mode [Figs. 3(a)-(c)], one can see that when w is small ($<10\ \text{nm}$), the N_{eff} and the MA are not significantly influenced by the SiO_2 thickness t . For $1 < t < 10\ \text{nm}$, the normalized MA keeps at ~ 0.12 , while the PL stays above $1\ \text{mm}$. As shown in Fig. 3(a), smaller MA can be achieved by increasing the core width w or decreasing the SiO_2 thickness. This indicates that when w

becomes large, the H_x^1 mode splits into “corner modes” due to the weakening of the field coupling in the x direction. The decoupling increases the N_{eff} [Fig. 3(b)] and therefore leads to a stronger confinement [8,10]. On the other hand, the decrease of the MA comes at the expense of a higher propagation loss. For example, for $t = 2$ nm and $w = 50$ nm, the normalized MA can be reduced to ~ 0.07 with a PL of ~ 60 μm . Such a PL is similar to that of a typical DLSPP waveguide, which, however, has a much larger normalized MA (~ 0.35) [4]. These results suggest that, by properly selecting the structural parameters, the H_x^1 mode can afford a good compromise between the tight confinement and the long-range propagation.

Different from the H_x^1 mode, the variation of w has little impact on the MA and N_{eff} of the H_y^1 mode [Figs. 3(d) and (e)] because the electric field is mainly concentrated in the top and bottom of the nanowire. For $w = 0$ (circular nanowires), the H_y^1 mode and the H_x^1 mode are degenerated with a 90° rotational symmetry of their polarization and the PL increases from 15 to 50 nm as t increases from 1 to 10 nm. When w becomes larger, the PL of the H_y^1 mode decreases, but the attenuation is much smaller than that of the H_x^1 mode. From Figs. 3(d) and (f), one sees that in the whole range of SiO₂ thickness and nanowire width, the H_y^1 mode can always achieve a $\sim 10^{-1}$ mode confinement with a >1 mm propagation distance, which is very helpful to the practical use.

It should be noted that for the minimum SiO₂ thicknesses considered in our study ($t = 1\sim 2$ nm), the results obtained based on Maxwell equations and bulk dielectric constants may not be accurate enough. For a more rigorous analysis, one needs to take quantum effects into account.

3. Crosstalk and input coupling efficiency

In order to evaluate the performance of the present waveguide in integrated circuits, we calculate the crosstalk between two parallel waveguides ($w = 20$ nm and $t = 5$ nm) by using the coupled mode theory. We consider two different arrangements: the parallel waveguides are aligned in the x direction [Fig. 4(a)], or in the y direction [Fig. 4(b)]. Figure 4 plots the coupling length as a function of waveguides separation D . One sees that the coupling lengths of the HOH modes are nearly 100 μm with a separation D of 800 nm. When D is increased to 1 μm , a coupling length of 1 mm can be achieved. Such a low crosstalk confirms the tight confinement ability of the proposed structure and is quite beneficial for improving the packing density. Contrarily, strong coupling happens when the waveguides are placed very close to each other. For instance, when $D = 500$ nm, the coupling length goes below 10 μm . This makes it useful in developing compact directional couplers [5].

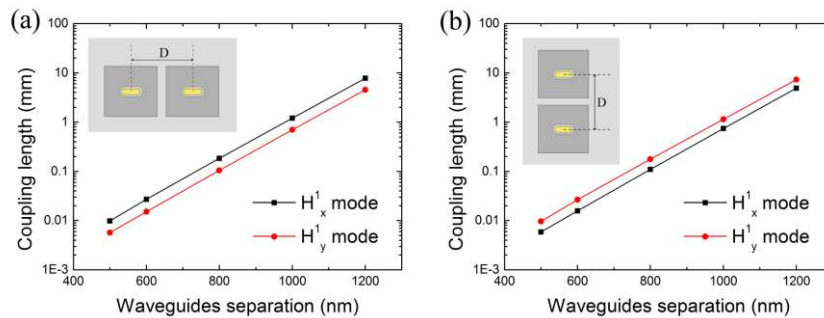


Fig. 4. Coupling length of parallel waveguides as a function of separation D .

Coupling efficiency between a dielectric waveguide and a plasmonic waveguide is another important issue. Previous studies have shown that most types of plasmonic waveguides suffer

from significant coupling loss because of their large mode mismatch with the existing dielectric waveguides [17–19]. For our hybrid structure, since the HOH modes have similar field orientation to that of the fundamental TE-like modes in the dielectric waveguides [denoted as E_x^0 and E_y^0 modes, see panel (i) of Fig. 5], one expects a better coupling efficiency. To verify this, a 3D-FEM simulation is implemented to calculate power transmission from a pure Si waveguide (lateral dimension: 400 nm × 400 nm) to a hybrid plasmonic waveguide ($w = 20$ nm, $t = 5$ nm). We define $z = 0$ as the coupling interface between the dielectric/plasmonic waveguides, and excite the fundamental dielectric modes at $z = -5$ μm. The mesh size in the z direction is set to be 5 nm near the coupling interface ($z = 0$) and 40 nm in the remaining computational domains.

Figure 5 depicts the evolution process of the electric field profile near the coupling interface. Mode coupling is observed close to $z = 0$, where the electric field gradually focuses into the SiO₂ layer and converts from the dielectric modes (panel (i) of Fig. 5) to the hybrid modes (panel (ii) of Fig. 5). The distance for the mode transformation is found to be less than 0.4 μm. One can see clearly that the E_x^0 mode transforms to the H_x^1 mode [Fig. 5(a)] while the E_y^0 mode transforms to the H_y^1 mode [Fig. 5(b)], which means the two HOH modes can be selectively excited through changing the polarization of the incident light. By calculating the ratio of the transmitted power flow at $z = 5$ μm and the input power flow at $z = -5$ μm, the coupling efficiency is found to be as high as ~90%. Such an excellent coupling efficiency is attributed to two reasons: first, the similarity of the field orientations and the match of the effective index between the two waveguide modes minimizes the interface reflection and then increases the transmission. Second, radiation loss is eliminated at the coupling point because the Si component of the hybrid waveguide has the same size as the access Si waveguide. Therefore, using the present structure, high-efficient coupling can be achieved without adding tapers or resonant cavities [19–21]. This simplifies the design and fabrication process.

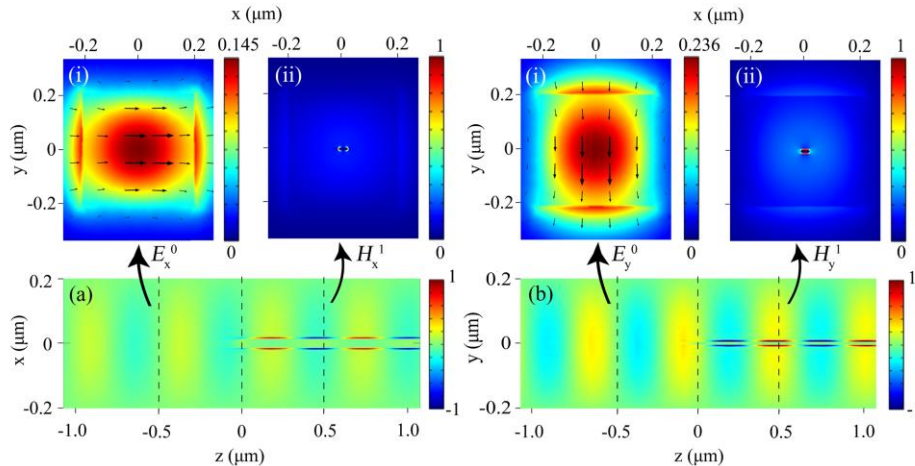


Fig. 5. Input coupling from a dielectric waveguide ($z < 0$) into a hybrid plasmonic waveguide ($z > 0$). (a) E_x field distribution of the H_x^1 mode in plane of $y = 0$. (b) E_y field distribution of the H_y^1 mode in plane of $x = 0$. The insets show the cross-sectional electric field amplitude $|E|$ at $z = -0.5$ μm and $z = 0.5$ μm. The arrows represent the orientation of the electric field.

4. Conclusion

We have proposed a new type of hybrid plasmonic waveguides which is constituted by embedding a SiO₂-covered silver nanowire into a Si waveguide. In contrast to the previous studies where the hybrid modes are caused by the coupling of the dielectric mode with the

fundamental plasmonic mode, here we have studied the high-order hybrid modes. Calculation shows that the hybrid modes have small mode areas, while the field orientation is analogous to that of the well-known LRSPP mode and enables the waveguide to achieve low-loss propagation, which is very helpful to construct compact components. In addition, we also demonstrate that the hybrid waveguide can be high-efficiently coupled with the conventional dielectric waveguide even without using additional coupling structures. These properties may facilitate the application of the present structure in high-density photonic integration.

Acknowledgments

This research was supported by the National Natural Science Foundation of China (Contract No. 10874119) and the Foundation for Development of Science and Technology of Shanghai (Grant No. 10JC1407200).